Supplemental Information

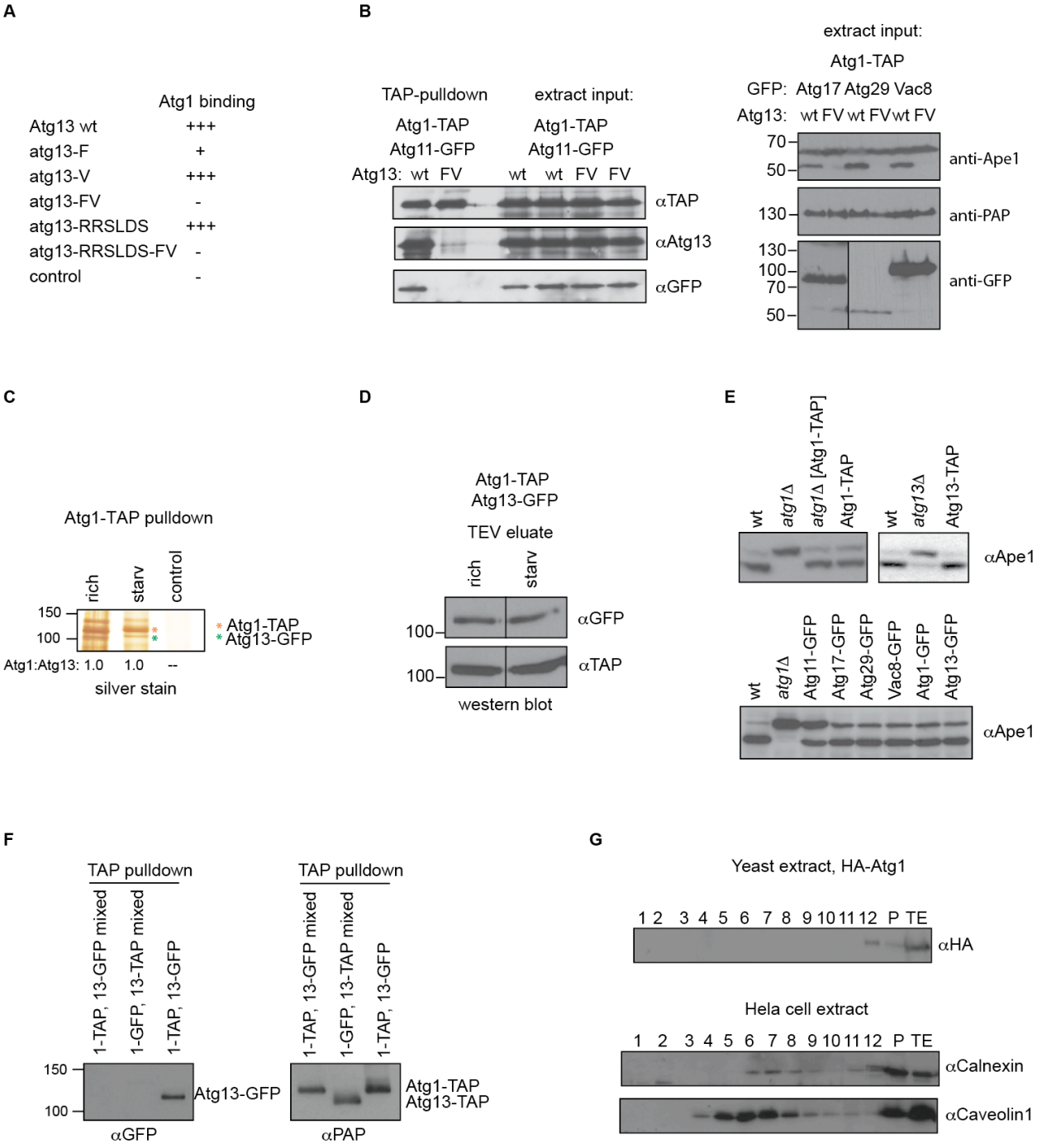

Figure S1

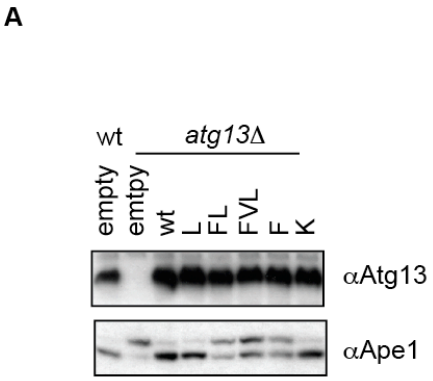

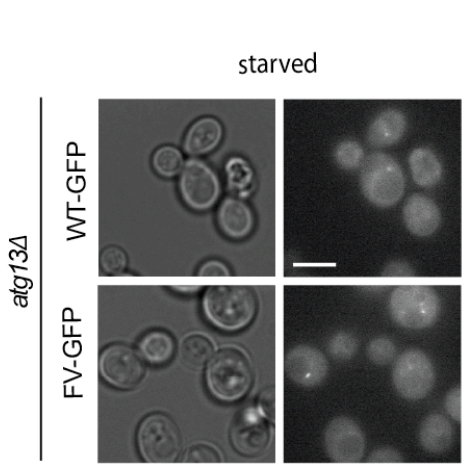

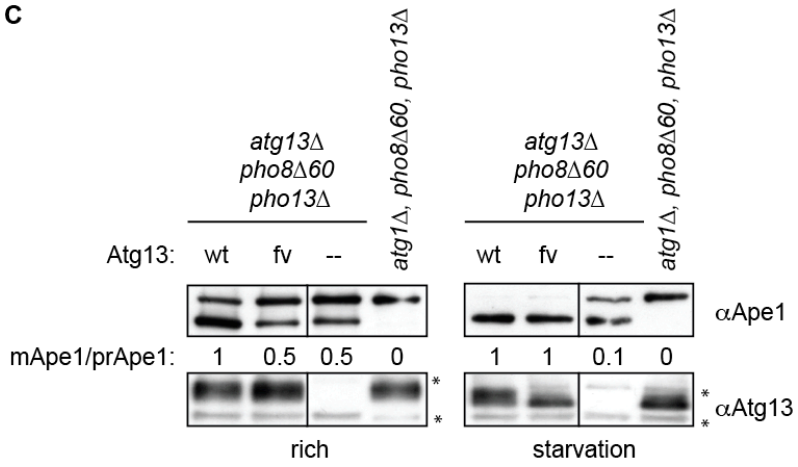

absolute ALP activity
[nmol p-nitrophenol/(min*mg)]

	rich		starvation	
Atg13:	mean	SD	mean	SD
wt	11.7	0.3	71.2	2.1
FV	10.7	0.4	14.5	0.5
--	10.1	0.6	10.5	0.4

Figure S2

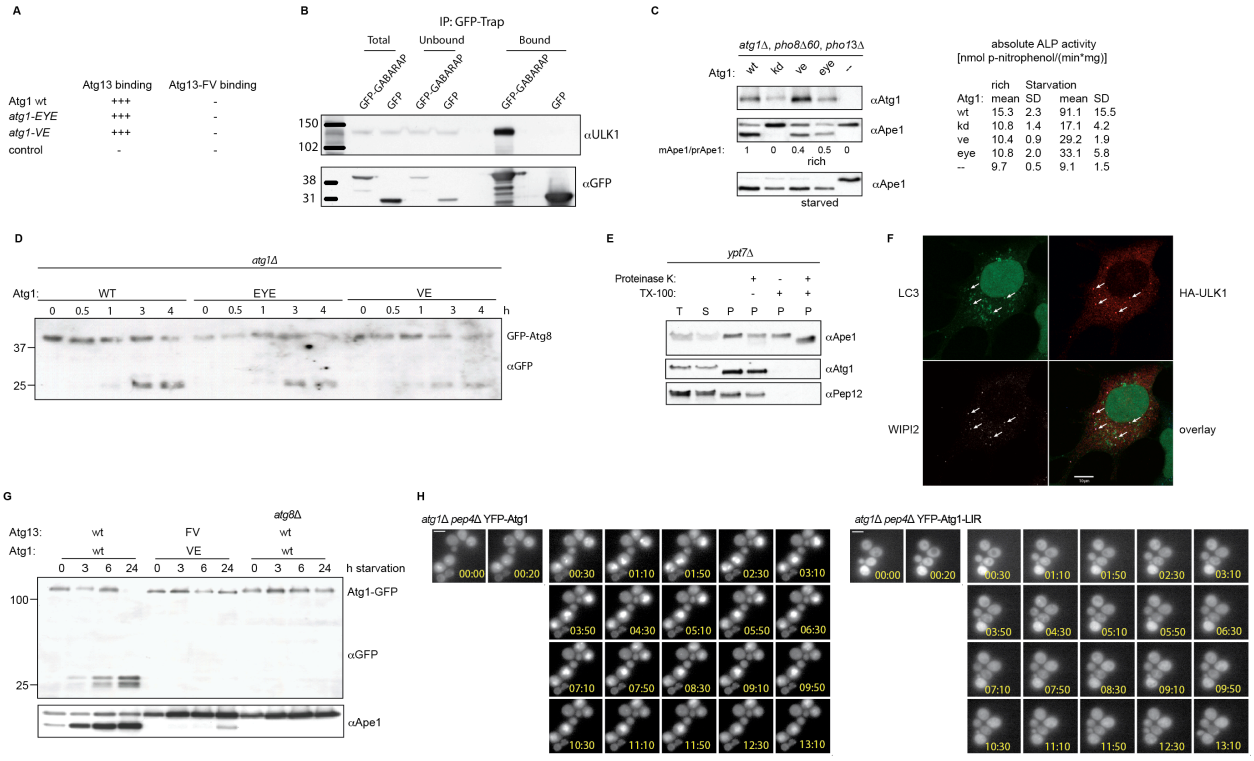

	Atg13 binding	Atg13-FV binding
Atg1 wt	+++	-
atg1-EYE	+++	-
atg1-VE	+++	-
control	-	-

Atg1:	rich mean	rich SD	Starvation mean	Starvation SD
wt	15.3	2.3	91.1	15.5
kd	10.8	1.4	17.1	4.2
ve	10.4	0.9	29.2	1.9
eye	10.8	2.0	33.1	5.8
--	9.7	0.5	9.1	1.5

Figure S3

Figure S1: F468 and V469 in Atg13 are required for Atg1 binding, and Atg1 and Atg13 do not artificially associate in extracts after cell lysis.

(a) The interaction of Atg1 with wild-type (wt) and the indicated Atg13 mutants was examined by two-hybrid analysis, and quantified by measuring β-galactosidase activity expressed by the LacZ reporter. (+++): strong interaction; (+): weak interaction; (-): no interaction. (b) *ATG1-TAP atg13Δ* cells containing endogenously tagged Atg11-GFP and wild-type (wt) or the Atg13 FV-mutant (F468A; V469A) were grown to mid log phase. Atg1 was immunoprecipitated and the association of Atg13 and Atg11-GFP was analyzed by immunoblotting (left panel). Extract input for Figure 1c (right panel; note that the GFP blot originates from the same gel, however, two different exposures were taken, separated by a black line). (c) Yeast cells containing endogenously tagged Atg1-TAP were grown to mid log phase and starved for 4 hours in SD-N medium. Atg1-TAP was affinity purified and subjected to SDS-PAGE and silver staining. Bands were identified by mass spectrometry. (d) Atg1-TAP immunoprecipitates from Figure 1e were TEV cleaved and the eluate was analyzed by western blotting. Lanes shown originate from the same gel at the same exposure. (e) TAP- and GFP-tagged strains were tested for their functionality measuring Ape1 processing. Note that Ape1 processing is slightly decreased in the Atg11-GFP strain. (f) Yeast cells expressing as indicated endogenously-tagged Atg1-TAP, Atg13-TAP, Atg1-GFP or Atg13-GFP, and a strain containing Atg1-TAP and Atg13-GFP were grown to mid log phase in separate cultures. Equal numbers of Atg1-TAP cells were then mixed with Atg13-GFP cells, and Atg13-TAP cells with Atg1-GFP cells. Extracts were prepared, followed by affinity purification of Atg1 or Atg13 via their TAP tags. Co-precipitating proteins were monitored by western blotting with anti-GFP and anti-PAP antibodies. Note that no Atg1-

Atg13 complexes were artificially assembled after cell lysis. (g) Extracts prepared from exponentially growing wild-type cells expressing HA-tagged Atg1 were floated in a 5–35% sucrose density gradient in 1% TX-100. Fractions were collected and analyzed by western blotting. TE: total extract, P: pellet fraction. Flotation of cytoplasmic calnexin or membrane-associated caveolin in HeLa cell extracts were included as technical controls.

Figure S2: Mutation of F468 and V469 in Atg13 reduces autophagic function but doesn't alter PAS association.

(a) *atg13Δ* cells containing either an empty control plasmid (empty), or plasmids expressing wild-type or the indicated Atg13 mutants (F468A, V469A, K470A, L471A) were grown to mid log phase, and processing of endogenous Ape1 was analyzed by western blotting. (b) *atg13Δ c*ells containing GFP-tagged wild-type Atg13 or the FV mutant were grown to mid log phase and starved for 4 hours in SD-N. Cells were analyzed by phase contrast (left images) and fluorescence microscopy (right images). Bar = 5μm. (c) Left panel: extracts from the pho8Δ60 assays in Figure 1h were analyzed for Ape1 processing. The asterisks indicate non-specific bands detected by the Atg13 antibody. Lanes shown originate from the same gel at the same exposure. Right panel: absolute values of alkaline phosphatase (pho8Δ60) specific activity presented in Figure 1F. The unit of specific activity of ALP is expressed in nmol of *p*-nitrophenol (product) formed by ALP under given experimental conditions per minute, per milligram of total protein extract.

Figure S3: Binding, Atg8-processing and vacuolar degradation of Atg1 upon starvation.

(a) The interaction of wild-type Atg1, Atg1-EYE and Atg1-VE with wild-type Atg13 and the Atg13-FV mutant was measured by two-hybrid analysis. An empty plasmid was included for control. (+++): strong interaction; (-): no interaction. (b) HEK293 cells were transfected with GFP or GFP-GABARAP, and binding of endogenous ULK1 (upper panel) was analyzed by western blotting after immunoprecipitation with GFP-Trap resin. Immunoblotting with GFP antibodies (lower panel) controls for the presence of GFP and GFP-GABARAP. (c) Left panel: extracts from the pho8Δ60 assays shown in Figure 3B were analyzed for Ape1 processing. Right panel: Absolute values of alkaline phosphatase (pho8Δ60) specific activity presented in Figure 3B. The unit of specific activity of ALP is expressed in nmol of p-nitrophenol (product) formed by ALP under given experimental conditions per minute, per milligram of total protein extract. (d) *atg1Δ* cells expressing either wild-type Atg1, Atg1-EYE or Atg1-VE were grown to mid log phase and then starved for 4 hours in SD-N. Samples were taken at indicated time points and the processing of GFP-Atg8 was analyzed by anti-GFP western blotting. (e) Exponentially growing *ypt7Δ* cells were starved in SD-N medium for 4 hours, lysed and the extract separated into a cytoplasmic (S) and a 5'000xg membrane pellet (P) fraction. The pellet was treated with proteinase K in the presence or absence of TX-100 and analyzed by western blotting with anti-Atg1, anti-Ape1 and anti-Pep12 antibodies. Note that in the absence of protease inhibitors Atg1 is degraded by intracellular proteases released by TX-100 (compare lane 5: no inhibitors, and Figure 4A lane 5: with inhibitors). (f) HEK293 cells stably expressing GFP-LC3 were transfected with HA-ULK1, starved for 2 hours the next day and

subsequently immunostained for HA (red) and WIPI2 (white). (g) *atg1Δatg13Δ* or *atg8Δ* cells containing as indicated either GFP-tagged wild-type Atg1 or the Atg1-VE mutant, and wild-type Atg13 or the Atg13-FV mutant were grown to mid log phase followed by starvation for 24 hours in SD-N medium. Samples were taken at the indicated time points and GFP cleavage was analyzed by western blotting. Processing of endogenous Ape1 under starvation conditions analyzed by western blotting monitors autophagic flux. (h) *atg1Δpep4Δ* cells containing YFP-tagged Atg1 wild-type or the Atg1-VE mutant were grown to log phase and starved in SD-N medium. Cells were monitored by time-lapse microscopy (time in minutes, e.g. “1:30” indicates the cells have starved for 1h and 30 minutes). Bar = 5μm.

Table S1: Yeast strains used in this study.

Name	Genotype	Background	Source
yCK566	Mat a;	S288C	Euroscarf
yCK486	Mat a; atg13-GFP:HisMX6; atg1-TAP:HisMX6	S288C	this study
yCK489	Mat alpha; atg13::kanMX6; atg1-TAP:HisMX6		
yCK707	Mat a; atg1-TAP:HisMX6; atg13::kanMX6; Vac8-GFP:HisMX6	S288C	this study
yCK490	Mat a; atg1::kanMX6; atg13::kanMX6	S288C	this study
yCK418	Mat a; atg13::kanMX6	S288C	this study
yCK660	Mat a; atg1::kanMX6	S288C	(Kijanska et al, 2010)
yCK675	Mat a; atg1::kanMX6; atg8::natMX6	S288C	this study
yMK108	Mat a; atg1::kanMX6; pep4::natMX6	S288C	this study
yCK5	Mat a; atg1-TAP:HisMX6	S288C	Euroscarf
yCK8	Mat a; atg13-GFP:HisMX6	S288C	Euroscarf
yCK6	Mat a; atg1-GFP:HisMX6	S288C	Euroscarf
yCK7	Mat a; atg13-TAP:HisMX6	S288C	Euroscarf
yCK31	Mat a; pep4::natMX6	S288C	this study
yMK105	Mat a; atg1::kanMX6;ypt7::natMX6	S288C	this study
BY4741	Mat a; his3Δ1; leu2Δ0; met15Δ0;ura3Δ0	S228C	Euroscarf
yMK117	Mat a; atg13::natMX6, pho8::pho8Δ60:HisMX6, pho13::kanMX6	S288C	this study
yMK112	Mat a; atg1::natMX6, pho8::pho8Δ60:HisMX6, pho13::kanMX6	S288C	this study
yMK122	Mat alpha; atg1-TAP: HisMX6, atg17-GFP:hisMX6, atg13::kanMX6	S288C	this study
yMK124	Mat a; atg1-TAP: HisMX6, atg29-GFP:hisMX6, atg13::kanMX6	S288C	this study
yCK864	Mat a; atg1-TAP: HisMX6, atg11-GFP:hisMX6, atg13::kanMX6, MET15	S288C	this study
yCK587	Mat a; atg13-TAP: HisMX6, atg1::kanMX6	S288C	this study
yCK534	Mat a; atg11-TAP: HisMX6	S228C	Euroscarf
yCK535	Mat a; atg17-TAP: HisMX6	S228C	Euroscarf
yCK538	Mat a; atg29-TAP: HisMX6	S228C	Euroscarf
yCK540	Mat a; vac8-TAP: HisMX6	S228C	Euroscarf

The genotype of *S.cerevisiae* S288C genetic background used in this study is Mat a or Mat alpha; his3Δ1; leu2Δ0; met15Δ0;ura3Δ0.

Table S2: Plasmids used in this study.

Name	Characteristics	Source
pRS315	*CEN LEU2*	(Sikorski & Hieter, 1989)
pRS316	*CEN URA3*	(Sikorski & Hieter, 1989)
pCK113	*pRS316; ATG13*	this study
pCK219	*pRS316; atg13* $^{F468A,\ V469A}$	this study
pCK320	*pRS315; ATG1-TAP*	this study
pCK48	*pRS315; GFP-ATG8*	this study
pCK394	*pRS315; atg1* $^{V432A,\ E433A}$*-TAP*	this study
pCK387	*pRS315; atg1* $^{E428A,\ Y429A,\ E433A}$*-TAP*	this study
pCK424	*pRS315; atg1* $^{E428A,\ Y429A,}$ *-TAP*	this study
pCK111	*pRS315; ATG1*	(Kijanska et al, 2010)
pCK353	*pRS315; atg1* $^{E428A,\ Y429A,\ E433A}$	this study
pCK352	*pRS315; atg1* $^{V432A,\ E433A}$	this study
pMK102	*pRS313; GFP-ATG8*	this study
pCK35	*pRS313; APE1-RFP*	(Meiling-Wesse et al, 2005)
pCK319	*pRS315; ATG1-GFP*	this study
pMK108	*pRS315; atg1* $^{V432A,\ E433A}$*-GFP*	this study
pCK346	*pRS315; atg1* ^{K54A}*-TAP*	this study
pMK107	*pRS315; atg1* ^{T226A}*-GFP*	this study
pMK112	*pRS416; ATG13-GFP*	this study
pCK14	*pRS316; YFP-ATG1*	(Suzuki et al, 2001)
pCK568	*pRS316; YFP-atg1* $^{V432A,\ E433A}$	this study
pCK120	*pRS416; 3HA-ATG1*	(Kijanska et al, 2010)
pCK378	*pRS316; atg13* ^{F468A}	this study
pCK389	*pRS316; atg13* ^{L471A}	this study
pCK390	*pRS316; atg13* $^{F468A,\ L471A}$	this study
pCK391	*pRS316; atg13* $^{F468A,\ V469A,\ L471A}$	this study
pCK392	*pRS316; atg13* ^{K470A}	this study
pMK110	*pRS415; ATG13-GFP*	this study
pMK111	*pRS415; atg13* $^{F468A,\ V469A}$ *-GFP*	this study
pCK181	*pLexA-N; ATG13*	(Kijanska et al, 2010)
pCK309	*pLexA-N; ATG13* $^{F468A,\ V469A}$	this study
pCK202	*pGAD-HA; ATG1*	(Kijanska et al, 2010)
pCK84	*pGAD-HA*	Dual Systems
pCK430	*pGAD-HA; atg1* $^{E428A,\ Y429A,\ E433A}$	this study
pCK432	*pGAD-HA; atg 1* $^{V432A,\ E433A}$	this study
pCK86	*pLexA-N*	Dual Systems
pCK191	*pLexA-N; ATG13-432-520*	(Kijanska et al, 2010)
pCK339	*pLexA-N; atg13-432-520* ^{F468A}	this study
pCK305	*pLexA-N; atg13-432-520* ^{V432A}	this study
pCK293	*pLexA-N; atg13-432-520* $^{F468A,\ V469A}$	this study
pCK206	*pLexA-N; atg13-432-520* ^{RRSLDS}	this study
pCK212	*pLexA-N; atg13-432-520* $^{RRSLDS-FV}$	this study
pcDNA3.1(+)HA-Ulk1	*HA-tagged human ULK1*	Image Clone
pcDNA3.1(+)HA-Ulk1(EYE)	*HA-tagged human ULK1* $^{D356A,\ F357A,\ P361A}$	this study

pEGFPC1-GABARAP	*GFP-tagged GABARAP*	Zvulun Elazar
pCK613	*pGEX4T-1; GST-atg1-501-897*	this study
pCK612	*pGEX4T-1; GST-atg13wt-432-520*	this study
pCK611	*pGEX4T-1; GST-atg13fv-432-520*	this study
IC60	*YCp111; pbs2-Suv320*	this study
IC92	*YCp111; atg13wt-Suv320*	this study
pLW13	*YCp111; atg13fv-Suv320*	this study
IC18	*YCp33; atg1-H3-HA*	this study

Supplementary References

Kijanska M, Dohnal I, Reiter W, Kaspar S, Stoffel I, Ammerer G, Kraft C, Peter M (2010) Activation of Atg1 kinase in autophagy by regulated phosphorylation. *Autophagy* **6:** 1168-1178

Meiling-Wesse K, Epple UD, Krick R, Barth H, Appelles A, Voss C, Eskelinen EL, Thumm M (2005) Trs85 (Gsg1), a component of the TRAPP complexes, is required for the organization of the preautophagosomal structure during selective autophagy via the Cvt pathway. *J Biol Chem* **280:** 33669-33678

Sikorski RS, Hieter P (1989) A system of shuttle vectors and yeast host strains designed for efficient manipulation of DNA in Saccharomyces cerevisiae. *Genetics* **122:** 19-27

Suzuki K, Kirisako T, Kamada Y, Mizushima N, Noda T, Ohsumi Y (2001) The pre-autophagosomal structure organized by concerted functions of APG genes is essential for autophagosome formation. *Embo J* **20:** 5971-5981